

Isothermal titration calorimetry

Ernesto Freire, Obdulio L. Mayorga, and Martin Straume

Anal. Chem., 1990, 62 (18), 950A-959A • DOI: 10.1021/ac00217a002

Downloaded from <http://pubs.acs.org> on January 2, 2009

More About This Article

The permalink <http://dx.doi.org/10.1021/ac00217a002> provides access to:

- Links to articles and content related to this article
- Copyright permission to reproduce figures and/or text from this article



ACS Publications

High quality. High impact.

Analytical Chemistry is published by the American Chemical Society. 1155 Sixteenth Street N.W., Washington, DC 20036

Isothermal Titration

Ernesto Freire, Obdulio L. Mayorga¹, and Martin Straume
Biocalorimetry Center
Department of Biology
The Johns Hopkins University
Baltimore, MD 21218

Calorimetric techniques have contributed a great deal to our current understanding of the mechanisms of regulation and control of biological structures and processes at the molecular level. Over the past decade and a half, advances have been made in both the development of highly sensitive microcalorimetric instrumentation and the development of analytical procedures to extract thermodynamic information about biological systems (see References 1–4 for reviews).



The principal calorimetric techniques that have contributed this information are differential scanning calorimetry (DSC) and isothermal titration calorimetry (ITC). By applying DSC, researchers have learned about the nature and magnitude of the forces that stabilize biological macromolecules (such as proteins and nucleic acids) and macromolecular assemblies (lipid bilayers, protein-lipid complexes, and protein-nucleic acid complexes). Accurate determination of the energy of stabilization of these biological structures by DSC has made possible elucidation of mechanistic details regarding interactions between regions within macromolecules and among components in multimolecular assemblies. DSC experiments involve perturbing the system under study by varying the thermal energy content of the sample (i.e., by scanning temperature as the independent variable under experimental control). The heat capacity of the system is then measured against temperature as the direct thermodynamic observable (recall that the heat capacity is the temperature deriv-

ative of enthalpy).

In contrast, ITC measures the energetics of biochemical reactions or molecular interactions (ligand-binding phenomena, enzyme–substrate interactions, and interactions among components of multimolecular complexes) at constant temperature. In this case, reaction is triggered by changing the chemical composition of the sample by titration of a required reactant. The heat associated with the reaction is the direct thermodynamic observable (related to both the enthalpy and extent of reaction). In an ITC experiment, the total concentration of reactant is therefore the independent variable under experimental control.

Because the majority of biological reactions can be induced isothermally, the potential range of applications of

attracted the attention of many investigators in recent decades. Throughout the years, biologists have studied these processes using a variety of experimental techniques and analytical methods to obtain accurate descriptions of their equilibrium behavior.

Several parameters must be included in the description of binding or association equilibria. First is the number of binding sites or stoichiometry of the reaction. Second is the strength of the association, usually expressed in terms of the association constant, K_a , or the Gibbs free energy of association, $\Delta G = -RT \ln K_a$. Third is the characterization of multiple sites and positive or negative cooperative interactions for those cases in which more than one binding site is present. Fourth is the characterization of the enthalpic and

ITC far exceeds that of DSC. However, until recently, the use of ITC has been limited because of a lack of sufficient sensitivity. The situation has changed with the recent development of instruments capable of measuring heat effects arising from reactions involving as little as nanomole amounts of reactants (5–11). This new generation of titration calorimeters makes possible direct thermodynamic characterization of association processes exhibiting very high affinity binding constants (10^8 – 10^9 M^{-1}) that are frequently found in biological reactions (5–11).

In this article we will present an overview of ITC and recent advances in ITC technology, discuss future directions for further evolution and application of ITC to biomedical research, outline the mathematical treatment of data for some simple binding models, and describe some recent applications of ITC to systems of biological interest.

Binding equilibrium

The association of biological macromolecules with one another as well as their association with small ligand molecules plays a central role in the structural assembly and functional regulation of biological systems and thus has

entropic contributions to the Gibbs free energy of association ($\Delta G = \Delta H - T\Delta S$). Fifth is the characterization of the dependence of the binding equilibrium on other environmental variables such as pH, ionic strength, and so forth. Most experimental techniques and analytical methods for binding studies are designed to evaluate these different parameters.

Two different approaches are normally used to study the binding equilibrium between two molecules. One approach relies on the direct measurement of the concentrations of free and bound ligand molecules using a technique such as equilibrium dialysis. The other approach takes advantage of the existence of changes in physical observables that are proportional to the extent of binding saturation. The binding of oxygen to hemoglobin, for example, causes changes in the optical absorbance in the Soret region (~420 nm) of hemoglobin (12–14). The magnitude of these changes is proportional to the degree of saturation and has been used extensively in the analysis of this binding process (12–14).

Calorimetric titration, which belongs to this second type of approach, measures the heat released or absorbed by

¹ Permanent address: Department of Physical Chemistry, University of Granada, Granada, Spain

Calorimetry

the stepwise addition of a ligand molecule to a solution containing the macromolecule under study. In general, whatever the approach used to examine binding, the goal is to generate a binding isotherm, a curve that represents the degree of saturation in terms of the ligand concentration. In ITC, the degree of saturation is defined in terms of the heat associated with the reaction.

Throughout the years, different mathematical procedures have been devised to estimate association constants, numbers of binding sites, and cooperative interactions from ligand-binding isotherms. In this respect, the analysis of calorimetrically determined binding isotherms follows the same principles. Among biologists, linearized representations of the data have

ciation constant. Use of the relation $\Delta G = -RT \ln K = \Delta H - T\Delta S$ allows further calculation of the entropy change. Thus a single calorimetric titration provides a complete characterization of the energetics of binding. In contrast, estimation of enthalpy and entropy changes using noncalorimetric techniques requires several binding experiments at multiple temperatures and subsequent analysis of the temperature dependence of the association constant. Calorimetry is unique because it provides direct measurement of the thermodynamic quantities of interest.

What is ITC?

With ITC, one measures directly the energetics (via heat effects) associated with reactions or processes occurring at

reactions could be obtained only for reactions exhibiting ligand association constants of 10^4 M^{-1} or less because sufficiently low reactant concentrations could not be examined to determine higher affinity binding constants. For those binding reactions with $K_a > 10^4 \text{ M}^{-1}$, only overall binding enthalpies, but not binding constants, could be determined directly from calorimetric titrations (some other method was required to determine K_a).

Over the years, technologies and instrument designs have evolved to produce isothermal titration calorimeters with much improved capabilities for detection of ever smaller heat effects. Such efforts during the 1980s led to the design and construction of titration microcalorimeters capable of measuring heat effects down to levels of 10^{-6} cal (5–11). The most significant of these developments have been those related to increasing the specific sensitivity and improving the time response of titration microcalorimeters. Because biomolecular association reactions are frequently characterized by very high binding constants (in the range of 10^8 M^{-1} or greater), experiments must be conducted under conditions of very dilute reactants (10^{-6} M or less) to accurately determine equilibrium constants as well as binding enthalpies. As such, a major goal in calorimetric design is optimization of the specific instrument sensitivity (heat per unit volume) rather than the absolute sensitivity.

Fundamental principles of isothermal titration calorimeter operation

Figure 1 is a schematic showing a differential, power compensation isothermal titration calorimeter (ITC-2) developed at the Biocalorimetry Center at The Johns Hopkins University. Detection of heat effects in this isothermal calorimeter is accomplished by use of semiconductor thermopiles interposed between the titration cells and a heat sink (a large metal mass in thermal equilibrium with a thermostatted water bath). Two titration cells reside in the calorimeter assembly; one acts as the reference and the other as the sample titration cell. When an ITC experiment is being performed, the reference cell contains buffer only and the sample cell contains buffer plus the reactant to which the injected material will be titrated.

Prior to beginning the experiment, the instrument's injection mechanism is filled with titrant, the titration cells are filled with the material to be titrated, and the calorimeter is equilibrated

Direct Thermodynamic Characterization of Biological Molecular Interactions

been widely used in the past. A particularly popular transformation has been the Scatchard plot, in which the ratio of the concentrations of bound and free ligand is plotted against the concentration of bound ligand. These transformations, however, usually introduce statistical biases in the analysis because they obscure the distinction be-

constant temperature. Experiments are performed by titration of a reactant into a sample solution containing the other reactant(s) necessary for reaction. After each addition, the heat released or absorbed as a result of the reaction is monitored by the isothermal titration calorimeter. Thermodynamic analysis of the observed heat effects

INSTRUMENTATION

tween dependent and independent variables.

In general, a more robust and statistically significant parameter estimation can be achieved by direct nonlinear least-squares analysis of the dependent versus independent variable. With the widespread availability of computers, the trend toward this type of analysis has gained popularity in recent years (15, 16) and this is the type we will discuss here.

The major advantage of titration calorimetry derives from the fact that the binding isotherms are defined in terms of the heats of reaction and as such they allow a direct estimation of enthalpy changes in addition to the asso-

then permits quantitative characterization of the energetic processes associated with the binding reaction.

Applications of ITC in the 1970s were directed toward characterization of the thermodynamics of enzyme-catalyzed reactions (17–19), ligand binding to macromolecules (20–23), and ligand- or pH-induced macromolecular conformational changes (24). However, reliable measurement of heat effects could be performed only at levels of 10^{-3} cal or greater (see References 25–27 for reviews). Because of these limits in sensitivity, only those biological reactions exhibiting relatively strong heat effects could be studied. Entire binding isotherms for ligand-binding

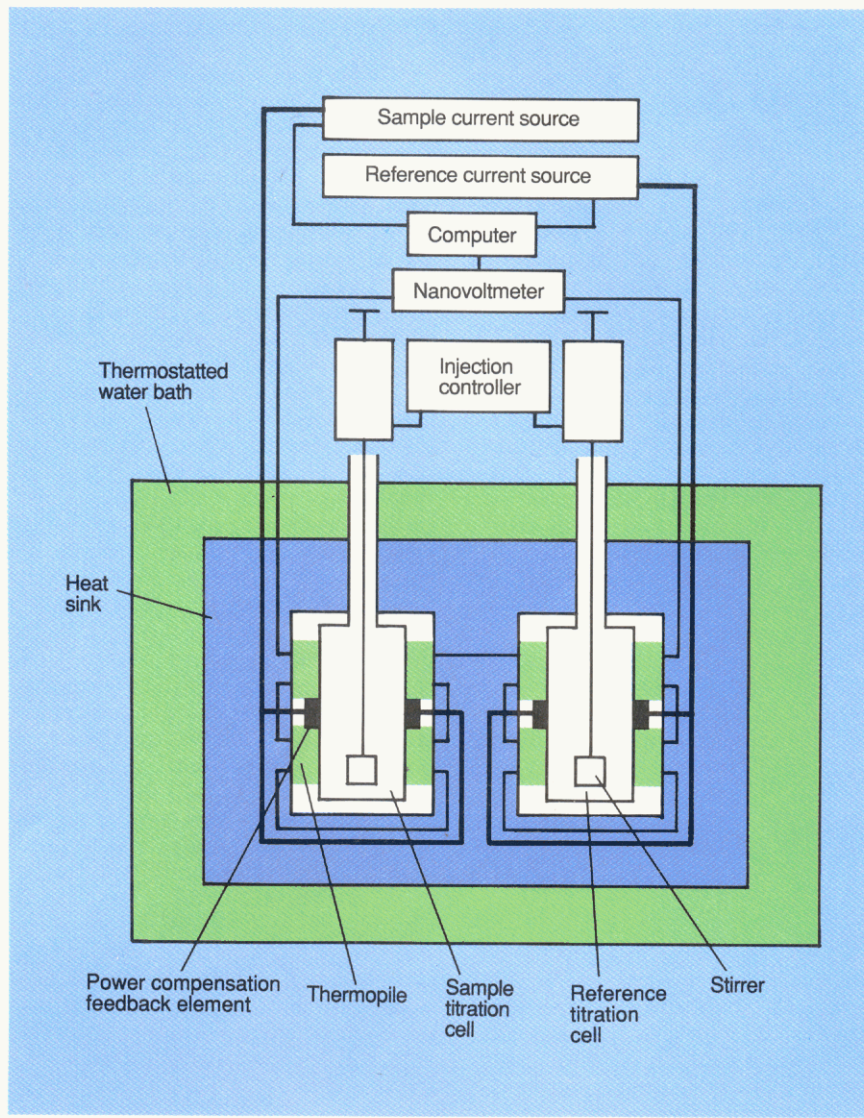


Figure 1. Schematic of the differential, power compensation isothermal titration calorimeter.

See text for operational details.

to the desired temperature such that all components of the instrument (i.e., titration cells, heat sink, and thermostatted water bath) have come to thermal equilibrium relative to each other. Identical injections of reactant are then introduced into both mechanically stirred titration cells by a dual-injection mechanism. The contents of the reference cell exhibit heat effects arising from injection and dilution of the reactant being titrated. The contents of the sample cell exhibit these same heat effects in addition to that associated with the reaction under study. Dual-injection isothermal titration calorimeters compensate in real time for both the heat effects arising from dilution of the injected reactant into the sample and for any mechanical heat effects arising from injection, yielding the heat of reaction of interest directly.

The titration cell compartments are constructed to permit heat flow between the titration cells and the heat sink only through the thermopile thermal detectors. The output of the thermopiles, an electrical potential (voltage), is directly proportional to the temperature difference across the faces of the thermopiles. This temperature difference, in turn, is proportional to the thermal power (rate of heat transfer [cal s^{-1}]) being exchanged between the titration cells and the heat sink. In the absence of power compensation, the time integral of this rate of heat transfer is the total heat of reaction induced in the respective titration cells as a result of injection.

Because the thermopiles of the sample and reference titration cells are connected in opposition electrically, the experimental quantity actually

monitored by this differential isothermal titration calorimeter is the difference in the rates of heat production or absorption between the sample cell and the reference cell. A nanovoltmeter measures the differential voltage output produced by the thermopiles and transmits this information to a computer interfaced for data acquisition and dynamic control of a power compensation mechanism. Power compensation is accomplished by continuously regulating the amount of heat applied to the titration cells so as to drive the temperature difference between the two cells toward the baseline, steady-state value.

The computer monitors the nanovoltmeter output (which is proportional to the temperature difference between the two titration cells) and adjusts the current applied to the cell feedback elements to compensate for the detected change in differential temperature between the cells. The applied thermal power as a function of time required to return the isothermal titration calorimeter to its steady-state temperature differential following an injection then becomes the experimentally determined quantity and is directly proportional to the heat of reaction of interest.

Increased intrinsic sensitivity

Very precise determination of temperature changes is necessary for reliable detection of heat effects on the order of 10^{-6} cal or less. The output of thermopile temperature detectors, as employed in the isothermal titration calorimeter developed in our laboratory and discussed here, is an electrical potential proportional to the temperature difference across the thermopiles. The magnitude of the voltage change per change in temperature is therefore an important consideration in instrument design so as to produce the maximum measurable response. During the past decade, semiconductor bismuth-telluride thermopiles have been introduced possessing 70 thermocouples (the individual temperature-sensing elements of thermopiles) per square centimeter. The use of thermopiles with a high density of thermocouple junctions per unit area provides enhanced voltage per degree response. The ITC-2 is equipped with 1056 of these junctions and is able to detect changes on the order of 10^{-8} cal s^{-1} (i.e., 40–50 nW) in thermal power.

Minimization of baseline noise is another factor important for improving isothermal titration calorimeter sensitivity levels. In the ITC-2 we have housed the titration calorimeter assembly in an ultrastable thermostat-

ted water bath to regulate temperature. Any fluctuations in bath temperature will transmit the temperature change via the heat sink to the titration cells and contribute to baseline noise, compromising instrument performance. The thermal damping effect provided by the mass of the metal heat sink in ITC-2 coupled with a stable thermostat capable of maintaining temperatures to within 10^{-6} – 10^{-5} °C over periods of minutes (and within 10^{-4} °C over 8 h) (28) has reduced the magnitude of baseline noise to a level on the order of 10^{-8} cal s $^{-1}$ (i.e., tens of nanowatts), thereby facilitating detection of small heat effects.

The ability to perform differential measurements of reference and sample responses in dual-injection instruments facilitates more accurate determination of heats of reaction. Because reaction is initiated in an ITC experiment by injection of a reactant, heat effects resulting from the mechanical disturbance of the injection event itself and dilution of the titrant are present in addition to the heat of reaction, which is the quantity of interest. A differential, dual-injection isothermal titration calorimeter compensates for these heat effects in real time. This eliminates the need for two separate experiments (a reference experiment to yield heats of injection and dilution and a sample experiment to exhibit

these effects and that of the reaction of interest) as required in a single-injection ITC (11).

Treatment of data obtained from single-injection ITC experiments involves subtracting these two individually observed responses to yield estimates of the heat of reaction of interest (11). Because they compensate in real time for any mechanical and dilution heat effects, dual-injection titration microcalorimeters capable of differential measurements do not introduce the additional error arising from consideration of two separate measurements.

Improved time response

The implementation of power compensation mechanisms some years ago has been a major factor in improving the time response of isothermal titration and differential scanning calorimeters and therefore in providing more accurate measurement of small heats of reaction (7). Because the total heat associated with a reaction is the time integral of the differential thermal power released or absorbed as a result of the reaction, reducing the time response is a means to more sensitive detection of total heat effects per injection. Heat conduction isothermal titration calorimeters passively transfer heat between the titration cell(s) and heat sink, giving rise to instrument time responses with lifetimes on the order of

100–300 s (8–10). The instrument discussed here uses continuous power compensation for active heat transfer and exhibits both considerably reduced instrument response times and improved signal-to-noise (S/N) characteristics. Active power compensation mechanisms, as introduced by McKinnon et al. (7), lead to reduced instrument response times and produce greater thermal power amplitude (the experimental observable) for equivalent heat effects. In other words, the S/N is increased as a result of the enhanced thermal power amplitude necessary to generate the same total observed heat signal (area under the thermal power versus time curve) in a shorter period of time before return to baseline.

This effect is demonstrated in Figure 2 in which the response signal of the instrument to identical 25 μ cal pulses is recorded for both the case in which power compensation is active and in which it is not (heat conduction mode). In both cases, the areas under the curves are identical but the signal deflection is approximately four times larger when power compensation is active. In the absence of power compensation, the instrument time response is 100 s whereas under power compensation conditions it is only 15 s. The recorded quantity in a power compensation titration calorimeter is the amount

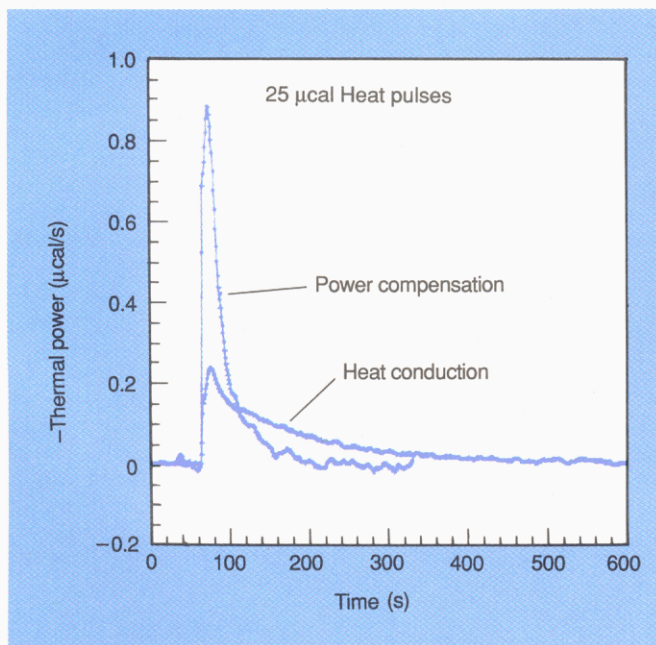


Figure 2. Power compensation vs. heat conduction modes of ITC-2 operation.

The observed differential thermal power vs. time response in the power compensation mode is distributed over a shorter period of time than that measured in the heat conduction mode. The amplitude of the thermal power response in the power compensation mode is greater than that detected in the heat conduction mode because of the more rapid instrument response.

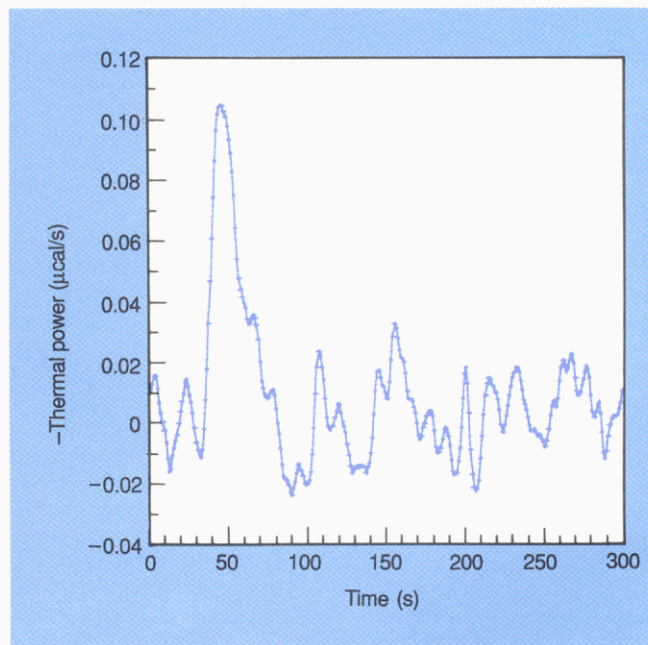


Figure 3. Differential thermal power vs. time response obtained from introduction of a $0.5 \mu\text{cal mL}^{-1}$ electrical calibration pulse into the sample titration cell of ITC-2 (sample contains 5 mL of water).

The maximum peak amplitude is 105 ncal s^{-1} ($21 \text{ ncal s}^{-1} \text{ mL}^{-1}$) with S/N sufficiently high to permit reliable measurements to considerably less than $1 \mu\text{cal mL}^{-1}$ event $^{-1}$.

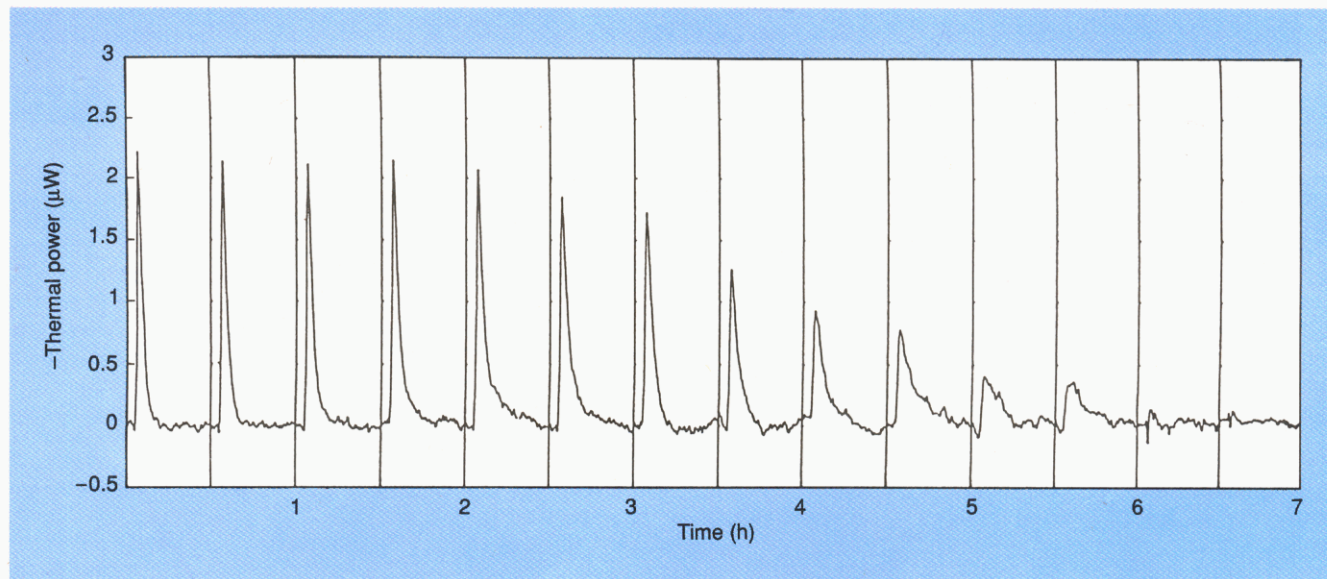


Figure 4. Isothermal calorimetric titration of cholera toxin B-subunit pentamer with oligo-G_{M1}, the oligosaccharide cell surface receptor for cholera toxin.

The differential power output in microwatts ($4.184 \mu\text{W} = 1 \mu\text{cal s}^{-1}$) is shown as a function of time and was obtained from successive injections of 3 nmol of oligo-G_{M1} (30-μL injections of 0.1 mM oligo-G_{M1}) into a solution of 4.9 nmol of B-subunit pentamer in 1.4 mL. (Reprinted from Reference 10.)

of thermal power that must be applied to compensate for the heat of reaction induced by injection. Because the instrument is both continuously monitoring the temperature differential (thermopile output) and continuously regulating the amount of applied thermal power (through the feedback elements) to actively return the system to the preinjection, steady-state temperature differential, the time required to obtain the total heat associated with the induced reaction is reduced.

In order to have the capability to compensate for exothermic and endothermic effects, a constant amount of thermal power is applied to both titration cells and a steady-state flux of thermal throughput from the cells to the heat sink is established. The amount of steady-state power applied to the cells is sufficiently small (0.5 mA of current through $\sim 230 \Omega$ of resistance, producing $14-15 \times 10^{-6} \text{ cal s}^{-1}$ of thermal power in 5 mL of cell volume) so that the overall temperature is not perturbed beyond the fluctuation regime of the thermostat. Compensation is accomplished by regulating the power introduced through the feedback elements (by changing the amount of applied current) in proportion to the change in thermopile output (detected change in temperature).

In addition to power compensation, the thin, disk-shaped gold titration cells used in the ITC-2 contribute to optimizing the response time. Positioning the walls of the titration cells in close opposition to each other minimizes the distance heat must travel

through the medium prior to encountering the thermopiles (which are in direct contact with the cell faces between the titration cells and heat sink). This design facilitates rapid detection of heat effects induced in the titration cell contents by injection of titrant.

Definitions used for reporting response times and noise levels vary in the literature and commercial documentation. Our definition of response time is the time required for decay of the thermal power amplitude to $1/e$ of its maximum value. Response times are frequently referred to, however, in the context of rise times to half maximal amplitude. By that definition, the ITC-2 has a response time of 3–4 s. In considering baseline noise levels, we report baseline noise as the standard deviation of the noise amplitude in individual baselines, in contrast to the standard error of reproducibility obtained from a large number of multiple, identical injections.

The differential, power compensation isothermal titration calorimeter described here currently has a limit of resolution of 10^{-6} cal of total heat. This represents a substantial improvement of approximately 3 orders of magnitude in sensitivity from the $\sim 10^{-3} \text{ cal}$ resolution in earlier reaction calorimeters. The titration cell volume is 5 mL, making the limit of specific sensitivity $\sim 0.2 \times 10^{-6} \text{ cal mL}^{-1}$.

An example of the limiting resolution of the instrument is presented in Figure 3, which shows its response to a pulse of $0.5 \times 10^{-6} \text{ cal mL}^{-1}$ ($2.5 \times 10^{-6} \text{ cal}$ total heat) introduced into the sam-

ple titration cell. The baseline noise level is $\pm 4-8 \times 10^{-9} \text{ cal s}^{-1}$ (standard deviation) or a peak-to-peak noise of $40 \times 10^{-9} \text{ cal s}^{-1}$ corresponding to a specific noise level of $\pm 0.8-1.6 \times 10^{-9} \text{ cal s}^{-1} \text{ mL}^{-1}$ (standard deviation) or a peak-to-peak specific noise of $8 \times 10^{-9} \text{ cal s}^{-1} \text{ mL}^{-1}$.

Analysis of ITC data

The function of many biological systems is modulated by ligand binding (e.g., binding of hormones or toxins to their target receptors, allosteric or feedback control of enzymes or other functional proteins, signal peptide-membrane interactions, and protein-nucleic acid interactions). Characterization of the energetics of such processes may be accomplished by ITC experiments. Upon binding of a ligand to a macromolecule (e.g., protein) or macromolecular assembly (e.g., multisubunit protein or membrane systems), heat will be released or absorbed accompanying the binding event (i.e., the enthalpy of ligand binding). The heat effects associated with each addition of ligand represent the experimentally observed response in an ITC experiment. For each injection, the heat released or absorbed is given by

$$q = V\Delta H\Delta[L_B] \quad (1)$$

where q is the heat associated with the change in bound ligand concentration, $\Delta[L_B]$ is the change in bound ligand concentration, ΔH is the enthalpy of binding ($\text{mol ligand})^{-1}$, and V is the reaction volume.

Because q is directly proportional to

the increase in ligand bound resulting from each injection, its magnitude decreases as the fractional saturation of the system is titrated stepwise to completion. This is illustrated in Figure 4 in which the B-subunit pentamer of cholera toxin is calorimetrically titrated with oligo-G_{M1}, the oligosaccharide binding region of its glycolipid cell surface receptor (see the section "Cholera toxin binding to oligo-G_{M1}" later in this article for more detail). The total cumulative heat released or absorbed is directly proportional to the total amount of bound ligand as

$$Q = V\Delta H \sum \Delta [L_B] = V\Delta H [L_B] \quad (2)$$

where Q is the cumulative heat and $[L_B]$ is the concentration of bound ligand.

Evaluation of calorimetric titration data as either individual or cumulative heat requires consideration of the heat evolved or absorbed as a function of total ligand added, or the total ligand concentration (the independent variable). Therefore, in the analysis of experimental data, the binding equations must be expressed in terms of the individual or cumulative heat released or absorbed as a function of total ligand concentration because these are the quantities experimentally known.

Multiple sets of independent binding sites

The most widely used theoretical framework for the analysis of binding data in biology is the so-called Multiple Sets of Independent Binding Sites model (for a complete review, see References 29 and 30). Within this framework, a macromolecule possesses an arbitrary number of sets of noninteracting binding sites. All of the sites in the same set possess the same intrinsic affinity for the ligand molecule. The great popularity of this model is due in part to its flexibility, which allows characterization of a large number of situations (See References 29 and 30 for some representative examples).

As expressed in Equation 1, the heat associated with the binding reaction is directly proportional to the concentration of bound ligand, $[L_B]$. For a system exhibiting multiple sets of independent binding sites, the concentration of ligand bound to each set is given by

$$[L_{B,i}] = [M] \frac{n_i K_i [L]}{1 + K_i [L]} \quad (3)$$

where $[L_{B,i}]$ is the concentration of ligand bound to binding sites of set i , $[M]$ is the total concentration of macromolecule available for binding ligand, K_i is the intrinsic site association constant

for binding sites of set i , n_i is the number of binding sites of set i on each macromolecule M, and $[L]$ is the concentration of free ligand.

The cumulative amount of heat released or absorbed as a result of ligand binding is given by the sum of the heats corresponding to each set as

$$\begin{aligned} Q &= V \sum_i \Delta H_i [L_{B,i}] \\ &= V[M] \sum_i \frac{n_i \Delta H_i K_i [L]}{1 + K_i [L]} \end{aligned} \quad (4)$$

where ΔH_i is the enthalpy of binding (mol ligand)⁻¹ to binding sites of set i . This equation can be expressed in terms of the total ligand concentration by way of the mass conservation expression $[L_T] = [L_B] + [L]$ (where $[L_T]$, $[L_B]$, and $[L]$ represent the total, bound, and free ligand concentrations, respectively). Analysis of calorimetric titration data is then performed by estimating the variable model parameters (n_i , K_i , and ΔH_i) by fitting either to the cumulative heat, Q , or to the individual heat, q (where the individual heat associated with the j -th injection event is q_j such that $q_j = Q_j - Q_{j-1}$). Analysis of data directly in terms of individual heats, q , is preferable because it eliminates propagation of the uncertainties associated with each successive injection that are necessarily present in cumulative heat data.

The two simplest cases are for one and two independent sets of ligand-binding sites. These cases allow explicit, closed-form expressions for Q as a

function of total ligand concentration as illustrated in Figures 5 and 6.

Figure 5 presents a schematic depiction and the closed-form equations characteristic of ligand binding to a macromolecule possessing one set of independent ligand-binding sites, the simplest special case of the general expression given by Equation 4. In the example depicted in this figure, the ligand-binding macromolecule possesses four independent and equivalent ligand-binding sites. Although $n = 4$ in this example, the expressions presented here are valid for any value of n . The open circles in the figure correspond to binding sites without bound ligand whereas the shaded squares represent binding sites with ligand bound. The binding constant, K , characterizes the affinity of each ligand-binding site for ligand L. The factors of 4, $\frac{3}{2}$, $\frac{2}{3}$, and $\frac{1}{4}$ are the particular statistical factors necessary to define the respective macroscopic equilibria for this case (i.e., $n = 4$) in terms of the site affinity constant, K .

The total cumulative heat, Q , is most conveniently expressed in terms of the free ligand concentration, $[L]$. However, the independent variable in ITC experiments is the total ligand concentration, $[L_T]$ (where $[L_T] = [L_B] + [L]$ and $[L_B]$ is the concentration of bound ligand). By recognizing that $[L_B] = Q/V\Delta H$ (where V is the reaction volume and ΔH is the binding enthalpy per mole of ligand), a closed-form expression is obtained for the cumulative heat, Q , in terms of the total ligand concentration, $[L_T]$. The energetics of a system obeying this model for ligand

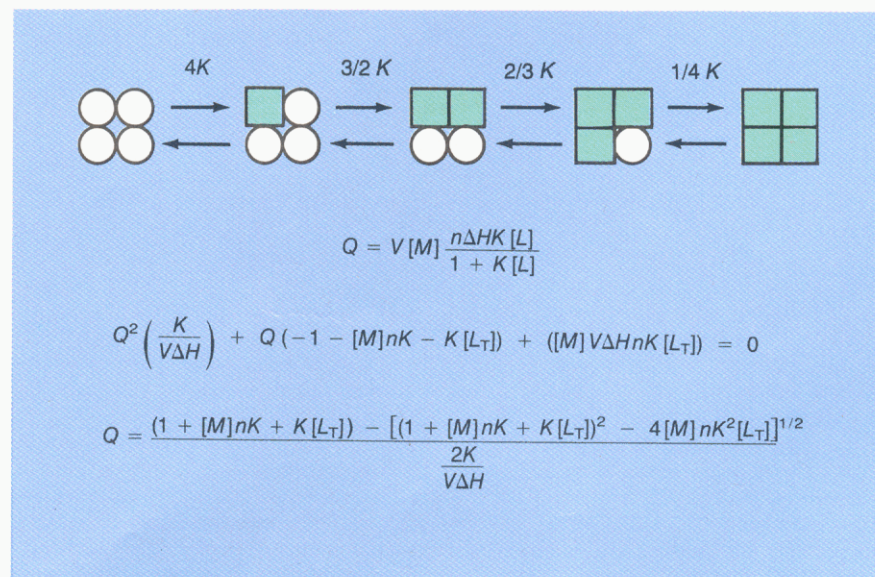


Figure 5. Schematic depiction and closed-form equations characteristic of ligand binding to a macromolecule possessing one set of independent ligand-binding sites. Shaded regions represent subunits to which ligand is bound. See text for a detailed description of relevant concepts.

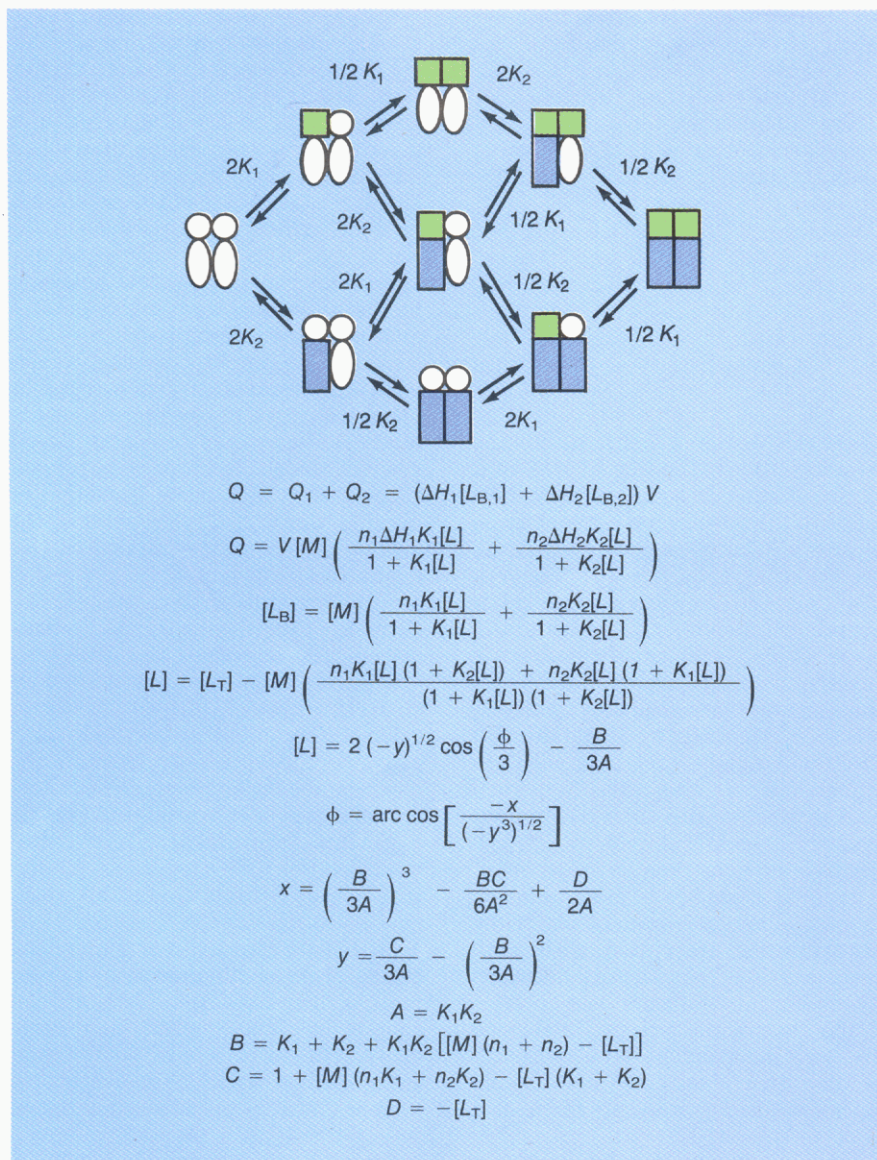


Figure 6. Closed-form equations for ligand binding to a macromolecule possessing two sets of independent binding sets.

Shaded regions represent subunits to which ligand is bound. See text for a detailed description of relevant concepts.

binding may therefore be considered in terms of $[L_T]$, $[M]$ (the total concentration of ligand-binding macromolecule), n , K , and ΔH for a known V .

This simple case is one of the few permitting such an explicit analytical solution. In general, a numerical approach is needed to express Q in terms of $[L_T]$. Estimation of the model parameters characteristic of this binding model (n , K , and ΔH) then requires fitting to either the cumulative heat, Q (i.e., $n_1 = 2$ and $n_2 = 2$) or to the individual heat, q .

Figure 6 shows the closed-form equations for ligand binding to a macromolecule possessing two sets of independent binding sites. This case is an extension of the model presented in Figure 5 according to the general expression of Equation 4 and permits

derivation of convenient closed-form expressions for the cumulative heat versus total ligand concentration. For illustrative purposes, this figure shows an example of a macromolecule possessing a total of four binding sites for ligand L , two of which have a site binding constant K_1 and the other two characterized by site binding constant K_2 (i.e., $n_1 = 2$ and $n_2 = 2$).

Even though the example in the figure uses $n_1 = n_2 = 2$, the equations in the figure are valid for any values of n_1 and n_2 . The open circles and ovals represent the two respective types of binding sites without ligands whereas the shaded squares and rectangles correspond to the respective types of sites with ligands. The factors 2 and $\frac{1}{2}$ are the statistical factors necessary to de-

fine the indicated macroscopic equilibria in this example in terms of the site binding constants, K_1 and K_2 (i.e., for the case where both n_1 and $n_2 = 2$).

The total cumulative heat, Q , will be composed of contributions from binding to each of the two sets of ligand-binding sites on the macromolecule, Q_1 and Q_2 . These, in turn, are related to the reaction volume, V , the respective site-binding enthalpies, ΔH_1 and ΔH_2 (per mole of bound ligand), and the concentrations of ligand L bound to the respective types of sites on the macromolecule, $[L_{B,1}]$ and $[L_{B,2}]$. Although the solution for this case is considerably more involved than that for the single-set-of-sites case (see Figure 5), expressions in terms of the total ligand concentration, $[L_T]$ (the independent variable in a titration experiment), may be obtained explicitly.

Cases in which more than two sets of binding sites are present cannot be solved in closed form and iterative numerical procedures must be used to solve Equation 4. In general, other situations like those in which cooperative interactions are present can be approached following the same philosophy, that is, development of the binding equations in terms of the total ligand concentration. For example, this approach has been used for the cooperative binding of cholera toxin to oligo-G_{M1}, the oligosaccharide binding region of its glycolipid cell surface receptor (10).

ITC applied to biological systems

We conclude this article by surveying some representative biological systems that have been studied by ITC.

Nucleotide binding to ribonuclease A. The detailed thermodynamic properties of 3'-cytidine monophosphate (3'CMP) binding to ribonuclease A (RNaseA) were studied in a comprehensive calorimetric titration study undertaken by Biltonen and co-workers in the 1970s (20, 21, 31, 32). Initial experiments were directed toward characterizing the fundamental thermodynamic binding properties of this system (Gibbs free energy, enthalpy, and entropy of interaction) in addition to binding stoichiometry and how these properties are influenced by salt concentration (20). In low-ionic-strength solution ($\mu = 0.05$ in either NaCl or KCl, pH 5.5), a binding stoichiometry of one 3'CMP bound per RNaseA molecule was found exhibiting $\Delta G = \sim -6.2$ kcal mol⁻¹ (corresponding to an association constant of 3.7×10^4 M⁻¹), $\Delta H = \sim -15.5$ kcal mol⁻¹, and $\Delta S = \sim -30$ cal K⁻¹ mol⁻¹ for the binding process.

The thermodynamic binding param-

eters varied in a continuous manner with increasing ionic strength until at $\mu = 3$ (in sodium acetate, pH 5.5), the ΔG for binding became less favorable to $\sim -4.5 \text{ kcal mol}^{-1}$ (corresponding to an association constant of $2.1 \times 10^3 \text{ M}^{-1}$) as a result of a considerably less favorable ΔH for binding (which became $\sim -6 \text{ kcal mol}^{-1}$) and despite a somewhat more favorable ΔS for binding ($\sim -5 \text{ cal K}^{-1} \text{ mol}^{-1}$).

Analysis of the enthalpic and entropic contributions to the free energy of protonation of the four histidine residues of RNaseA suggested that binding of 3'CMP is coupled to ionization of three of these residues. It has been suggested that the negative phosphate moiety of 3'CMP interacts electrostatically with two positively charged histidines and that interaction with the third (which shows an anomalously large enthalpy of protonation) involves a conformational rearrangement of the structure of RNaseA (21). The dependence on pH of the enthalpic and entropic contributions to the overall free energy of 3'CMP binding, when considered in conjunction with structural information, led to the conclusion that both van der Waals and electrostatic interactions contribute to binding but that the binding process is only weakly coupled to the conformational change associated with protonation of the histidine residues (31, 32).

Ligand binding and conformational transitions in human hemoglobin. The energetics associated with the binding of a variety of ligands to native and mutant human hemoglobins have been examined by application of titration calorimetric methods (33–36). By performing calorimetric titrations in buffers differing in their heats of protonation, the enthalpies of protonation of ionizable groups (histidines and/or α -amino groups) in response to oxygen, carbon monoxide, and inositol hexaphosphate (IHP) binding have been determined at different pHs. Enthalpies of carbon monoxide binding have been reported to be $\sim -23 \text{ kcal (mol CO)}^{-1}$ in the pH range from 6 to 9 (after correction for enthalpies of ionization of protein groups) (33).

These results were shown to be consistent with a model in which two ionizable histidines explain the origin of the Bohr proton effect. Interpretation of the relative enthalpic contributions of carbon monoxide binding and protein group ionization in a mutant and native human hemoglobin suggests that the enthalpy of protonation of ionizable protein groups is an important driving force for regulating heme site ligation as well as subunit association and hemoglobin tetramer conforma-

tional transitions.

The regulation of hemoglobin's functional properties is related to its ability to bind oxygen cooperatively. Calorimetric information from carbon monoxide-binding results obtained from a mutant hemoglobin (Hb M Iwate) and native hemoglobin, in conjunction with independent determinations of T-to-R transition free energies, suggests that the structural transition responsible for modifying the affinity of human hemoglobin for oxygen (the T-to-R transition, which gives rise to its cooperative oxygen-binding properties) is enthalpically controlled at pH 7.4 (with $\Delta H = 9 \pm 2.5 \text{ kcal mol}^{-1}$) but entropically controlled at pH 9 (with $\Delta H = -12 \pm 2.5 \text{ kcal mol}^{-1}$) (34).

The interaction of the regulatory ligand inositol hexaphosphate exhibits binding enthalpies of up to $\sim -25 \text{ kcal mol}^{-1}$ at pH 7.4 (after correction for buffer ionization effects). This binding corresponds to $\sim -11 \text{ kcal (mol H}^+ \text{ absorbed)}^{-1}$ associated with IHP binding. The binding of this regulatory ligand has therefore been concluded to be driven primarily by the exothermic protonation of histidine and/or α -amino groups as induced by the proximity of the negative phosphate charges on IHP (35, 36).

Signal peptide-lipid association. The interactions of the signal peptide of ornithine transcarbamylase with phospholipid vesicles of varying composition have recently been studied by isothermal titration calorimetry (9). It is the signal peptide sequences of newly translated mitochondrial proteins that have been recognized as being responsible for targeting and facilitating transport of these proteins into mitochondria. Because these sequences contain a large proportion of basic amino acids, they are expected to exhibit a strong interaction with the highly negative charged inner mitochondrial membrane. Titration of the signal peptide into phospholipid bilayers of surface charge density similar to that of the inner mitochondrial membrane reveals a strong binding characterized by an association constant on the order of 10^6 M^{-1} and an enthalpy change of $-60 \text{ kcal mol}^{-1}$.

The experiments were consistent with a binding stoichiometry of 1 peptide bound per 20 negatively charged phospholipid molecules. The magnitude of the binding constant indicates a strong membrane association, similar to that required for mitochondrial protein import and similar to that obtained from inhibition studies of the precursor protein (pre-ornithine transcarbamylase) by the synthetic signal sequence (37).

Cholera toxin binding to oligo-G_{M1}. Cholera toxin is a multisubunit protein consisting of a five-subunit ring, the B-subunit pentamer ($M_r = 58\,000$), which surrounds the dimeric A-subunit ($M_r = 27\,000$). The B-subunit pentamer binds to five ganglioside G_{M1} molecules on the outer surface of the cell membrane, and subsequently the A-dimer penetrates the cell membrane where it activates adenylate cyclase. The association of the B-subunit pentamer with the oligosaccharide region (oligo-G_{M1}) of the ganglioside triggers the sequence of events that leads to the release of the A-subunit from the B-subunit pentameric ring and its insertion into the interior of the membrane.

For many years it was known that the association of oligo-G_{M1} with the toxin exhibited positive cooperativity (38) even though the actual energetics and mechanism of this behavior remained difficult to elucidate by conventional techniques. These cooperative effects have their origin at the oligosaccharide-protein interface and result in the modification of the behavior of the pentameric ring (39) during membrane association, presumably facilitating the release of the A-subunit into the membrane interior.

Recently, the binding of oligo-G_{M1} was measured by isothermal titration calorimetry (10). These experiments also indicated positive cooperativity and allowed a complete mapping of intrinsic as well as cooperative interactions. The data were consistent with a nearest-neighbor model in which the binding of oligo-G_{M1} to one B-subunit enhances the affinity of adjacent B-subunits. The experiments yielded an intrinsic association constant of $1.05 \times 10^6 \text{ M}^{-1}$ at 37°C and a cooperative free energy of $-850 \text{ cal mol}^{-1}$. The magnitude of the cooperative free energy indicates a fourfold enhancement in the oligo-G_{M1} binding affinity of a B-subunit adjacent to a subunit to which oligo-G_{M1} is already bound. The intrinsic enthalpy change of binding was $-22 \text{ kcal (mol oligo-G}_{M1})^{-1}$ and the cooperative interaction enthalpy was $-11 \text{ kcal mol}^{-1}$.

The magnitude of the cooperative interaction enthalpy is consistent with a moderate structural "tightening" of the B-pentamer in agreement with spectroscopic data. Within the context of the cholera toxin-cell surface interaction, the cooperative enhancement has a twofold effect: It facilitates a complete (i.e., productive) attachment of the toxin to the membrane surface once the initial contact has occurred and it facilitates the release of the A-subunit into the interior of the mem-

brane through its associated conformational change.

Amino acid interactions with human plasminogen. A thermodynamic characterization by titration calorimetry of the binding of ϵ -amino caproic acid (EACA) to the isolated kringle 4 region (K4) of human plasminogen has recently been reported (40). Activation of human plasminogen is effected by the binding of α - and ω -amino acids. The K4 of human plasminogen is one of five highly homologous regions that are believed to be quite independent domains. These domains are believed to be the functionally significant structural components of plasmin(ogen) responsible for mediating interactions with substrates as well as with negative and positive effectors. Calorimetric titrations with EACA were consistent with a single-set-of-binding-sites model and produced model parameters of $n = 0.87$, $K_a = 3.82 \times 10^4 \text{ M}^{-1}$, $\Delta H = -4.50 \text{ kcal mol}^{-1}$, and $\Delta S = 6.01 \text{ cal K}^{-1} \text{ mol}^{-1}$ (40). The lack of a significant pH dependence on the thermodynamics of EACA binding (in the range from 5.5 to 8.2) suggested that titratable groups on K4 do not affect this binding interaction.

Further experiments with a series of structural analogues of EACA (3-amino-*o*propionic acid, 4-aminobutyric acid, 5-aminopentanoic acid, 7-aminoheptanoic acid, 8-aminoctanoic acid, *trans*-(4-aminomethyl)cyclohexane-carboxylic acid, and L-lysine) demonstrated that both the length of the hydrophobic region between the amino and ω -carboxyl groups of the ligand and ligand steric structural constraints are important factors in determining the affinity of interaction (40).

Calcium and magnesium binding to oncomodulin. The calcium- and magnesium-binding properties of oncomodulin, a calcium-binding protein found in a variety of tumor, transformed, and nonembryonic placental cells, have been thermodynamically characterized by direct binding studies and calorimetric titration experiments (41). Oncomodulin possesses two Ca^{2+} and/or Mg^{2+} binding sites. The first site binds either Ca^{2+} or Mg^{2+} ions and exhibits a much higher affinity for Ca^{2+} than Mg^{2+} ($K_a(\text{Ca}^{2+}) = 2.2 \times 10^7 \text{ M}^{-1}$, $K_a(\text{Mg}^{2+}) = 4.0 \times 10^3 \text{ M}^{-1}$). Calcium binding to this site is competitively inhibited by Mg^{2+} . The second site binds Ca^{2+} only, but with a lower intrinsic affinity than the first ($K_a = 1.7 \times 10^6 \text{ M}^{-1}$). Despite these differences in Ca^{2+} binding affinity, the exothermic Ca^{2+} binding enthalpies were the same for each site ($\Delta H = -4.52 \text{ kcal mol}^{-1}$) giving rise to different positive Ca^{2+} binding entropy changes for the two sites

($\Delta S = 18.4 \text{ cal K}^{-1} \text{ mol}^{-1}$ for the high affinity site and $\Delta S = 13.4 \text{ cal K}^{-1} \text{ mol}^{-1}$ for the low affinity site). Binding of Mg^{2+} is associated with an endothermic enthalpy change and an even more positive entropy change than that seen with Ca^{2+} binding to either site ($\Delta H = 3.1 \text{ kcal mol}^{-1}$ and $\Delta S = 26.5 \text{ cal K}^{-1} \text{ mol}^{-1}$).

The thermodynamics of ion binding to the Ca^{2+} - Mg^{2+} site are similar to those observed in parvalbumins, a family of structurally related Ca^{2+} and Mg^{2+} binding proteins that are believed to function simply as intracellular Ca^{2+} and Mg^{2+} buffers. The presence of a Ca^{2+} -specific site on proteins of this class, however, suggests that oncomodulin may function as a signal-transducing Ca^{2+} binding protein (41). The presence of such specific Ca^{2+} binding properties has been associated with other proteins of this class that are involved in signal transduction (e.g., calmodulin, troponin C, S100, calpains, squidulin, and Ca^{2+} vector protein) and is believed to provide a mechanism for inducing conformational changes that regulate interactions with target proteins in response to changes in intracellular Ca^{2+} (41). Comparison of the thermodynamics of Ca^{2+} binding to oncomodulin at its Ca^{2+} -specific site to that of calmodulin shows some interesting differences. Whereas modulation of the exposure of hydrophobic protein regions is suggested to be involved in the functional regulation of calmodulin by Ca^{2+} binding (because of the strong entropy-driven nature of the binding interaction), Ca^{2+} binding to oncomodulin may be primarily electrostatic in nature (because of the nearly equal favorable enthalpic and entropic contributions of Ca^{2+} binding) (41).

Conclusion

The ability to measure small heats of reaction on the order of 10^{-7} – 10^{-6} cal ($\text{mL of solution}^{-1}$) has opened the door to a direct thermodynamic characterization of many biological systems. Current sensitivity levels of isothermal titration microcalorimeters allow direct examination of binding processes exhibiting K_a s as high as 10^8 – 10^9 M^{-1} . High sensitivity is also important when considering structurally complex systems like biological membranes, intact cells, or other biological systems that are difficult to concentrate or obtain in relatively large amounts. The recent developments in ITC technology presented here together with parallel advancements in data analysis methods are permitting a direct calorimetric characterization of biological phenomena previously beyond the scope of this experimental technique.

References

- Biltonen, R.; Freire, E. *CRC Crit. Rev. Bioc.* 1978, 5, 85.
- Privalov, P. L. *Adv. Prot. Chem.* 1982, 35, 1.
- Freire, E. *Comments Mol. Cell. Biophys.* 1989, 6, 123.
- Privalov, P. L.; Tiktopulo, E. I.; Veniaminov, S., Yu.; Griko, Yu., V.; Makhatadze, G. I.; Khechinashvili, N. N. *J. Mol. Biol.* 1989, 205, 737.
- Spokane, R. B.; Gill, S. J. *Rev. Sci. Instrum.* 1981, 52, 1728.
- Donner, J.; Caruthers, M. H.; Gill, S. J. *J. Biol. Chem.* 1982, 257, 14826.
- McKinnon, I. R.; Fall, L.; Parody, A.; Gill, S. J. *Anal. Biochem.* 1984, 139, 134.
- Ramsay, G.; Prabhu, R.; Freire, E. *Biochemistry* 1986, 25, 2265.
- Myers, M.; Mayorga, O. L.; Emtage, J.; Freire, E. *Biochemistry* 1987, 26, 4309.
- Schon, A.; Freire, E. *Biochemistry* 1989, 28, 5019.
- Wiseman, T.; Williston, S.; Brandts, J. F.; Lin, L-N. *Anal. Biochem.* 1989, 179, 131.
- Mills, F. C.; Johnson, M. L.; Ackers, G. K. *Biochemistry* 1976, 15, 5350.
- Chu, A. H.; Turner, B. W.; Ackers, G. K. *Biochemistry* 1984, 23, 604.
- Doyle, M. L.; DiCera, E.; Gill, S. J. *Biochemistry* 1988, 27, 820.
- Straume, M.; Johnson, M. L. *Biochemistry* 1988, 27, 1302.
- Straume, M.; Johnson, M. L. *Biophys. J.* 1989, 56, 15.
- Goldberg, R. N. *Biophys. Chem.* 1975, 3, 192.
- Goldberg, R. N. *Biophys. Chem.* 1976, 4, 215.
- Johnson, R.; Biltonen, R. *J. Am. Chem. Soc.* 1975, 97, 2349.
- Bolen, D. W.; Flogel, M.; Biltonen, R. L. *Biochemistry* 1971, 10, 4136.
- Fogel, M.; Biltonen, R. L. *Biochemistry* 1975, 14, 2603.
- Atha, D. H.; Ackers, G. K. *Biochemistry* 1974, 13, 2376.
- Gaud, H. T.; Barisas, B. G.; Gill, S. J. *Biochem. Biophys. Res. Commun.* 1974, 59, 1389.
- Atha, D. H.; Ackers, G. K. *J. Biol. Chem.* 1971, 246, 5845.
- Eftink, M.; Biltonen, R. In *Biological Microcalorimetry*; Beezer, A. E., Ed.; Academic Press: New York, 1980; pp. 343–412.
- Barisas, B. G.; Gill, S. J. *Ann. Rev. Phys. Chem.* 1978, 29, 141.
- Langerman, N.; Biltonen, R. *Methods Enzymol.* 1979, 61, 261.
- Suurkuusk, J.; Wadso, I. *Chemica Scripta* 1982, 20, 155.
- van Holde, K. E. *Physical Biochemistry*, 2nd ed.; Prentice-Hall: Englewood Cliffs, NJ, 1985; Chapter 3.
- Cantor, C. R.; Schimmel, P. R. *Biophysical Chemistry, Part III: The Behavior of Biological Macromolecules*; W. H. Freeman: New York, 1980; Chapter 15.
- Fogel, M.; Biltonen, R. L. *Biochemistry* 1975, 14, 2610.
- Fogel, M.; Albert, A.; Biltonen, R. L. *Biochemistry* 1975, 14, 2616.
- Rudolph, S. A.; Gill, S. J. *Biochemistry* 1974, 13, 2451.
- Gaud, H. T.; Gill, S. J.; Barisas, B. G.; Gersonde, K. *Biochemistry* 1975, 14, 4584.
- Noll, L. A.; Gaud, H. T.; Gill, S. J.; Gersonde, K.; Barisas, B. G. *Biochem. Biophys. Res. Commun.* 1979, 88, 1288.
- Gill, S. J.; Gaud, H. T.; Barisas, B. G. *J. Biol. Chem.* 1980, 255, 7855.
- Gillespie, L. L.; Argan, C.; Taneja,

- A. T.; Hodges, R. S.; Freeman, K. S.; Shore, G. C. *J. Biol. Chem.* 1985, 260, 16045.
 (38) Sattler, J.; Schwartmann, G.; Knack, I.; Rohm, K. H.; Wiegandt, H. *Hoppe-Seyler's Z. Physiol. Chem.* 1978, 359, 719.
 (39) Goins, B.; Freire, E. *Biochemistry* 1988, 27, 2046.
 (40) Sehl, L. C.; Castellino, F. J. *J. Biol. Chem.* 1990, 265, 5482.
 (41) Cox, J. A.; Milos, M.; MacManus, J. P. *J. Biol. Chem.* 1990, 265, 6633.



Ernesto Freire is a professor in the Department of Biology and director of the Biocalorimetry Center at The Johns Hopkins University. He received B.S. and M.S. degrees in biochemistry from the University Cayetano Heredia, Lima, Peru, and a Ph.D.

in biophysics from the University of Virginia. His research work has been in the area of molecular biophysics, particularly in the development of new methods for the study of the energetics and thermodynamic mechanisms of protein folding, conformational equilibrium, and self-assembly of complex macromolecular systems.

and in the analysis of biological systems using calorimetric techniques.



Obdulio L. Mayorga is a visiting scientist in the Biocalorimetry Center at The Johns Hopkins University. He is a professor of physical chemistry at the University of Granada, Spain. He received a Ph.D. in physical chemistry from the University of Granada. His research work is in the area of calorimetric instrumentation development.

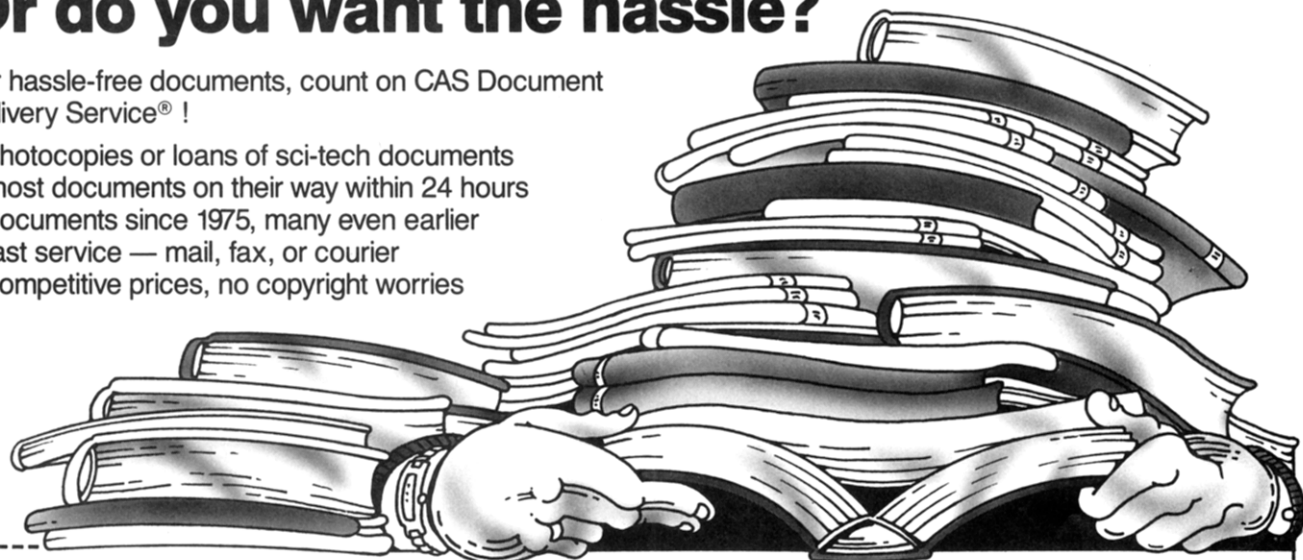


Martin Straume is the director of operations of the Biocalorimetry Center in the Department of Biology at The Johns Hopkins University. He received a B.S. degree in biochemistry and an M.S. degree in chemistry from Lehigh University and a Ph.D. in biochemistry from the University of Virginia. His research work has involved biophysical characterization of lipid-lipid and lipid-rhodopsin interactions, thermodynamic analysis of ligand binding to human hemoglobin, and development of high-sensitivity titration calorimetric instrumentation.

Do you want the document? Or do you want the hassle?

For hassle-free documents, count on CAS Document Delivery Service® !

- photocopies or loans of sci-tech documents
- most documents on their way within 24 hours
- documents since 1975, many even earlier
- fast service — mail, fax, or courier
- competitive prices, no copyright worries



Return this coupon to:

Chemical Abstracts Service

Marketing Dept. 33190

P.O. Box 3012

Columbus, OH 43210 U.S.A.

or call: 800-848-6538, ext. 2956 or
614-447-3670

fax: 614-447-3648

STNmail: CASDDSC

Name _____ Phone _____

Job Title _____

Organization _____

Address _____